Journal of Constructional Steel Research 87 (2013) 6–16

Contents lists available at SciVerse ScienceDirect

Journal of Constructional Steel Research

An experimental study on elliptical concrete filled columns under axial compression

N. Jamaluddin [a], D. Lam [b,*], X.H. Dai [b], J. Ye [c]

[a] Faculty of Civil and Environmental Engineering, Tun Hussein Onn University of Malaysia, Malaysia
[b] School of Engineering, Design and Technology, University of Bradford, Bradford, UK
[c] Department of Engineering, Lancaster University, Lancaster, UK

ARTICLE INFO

Article history:
Received 15 February 2013
Accepted 3 April 2013
Available online 4 May 2013

Keywords:
Concrete filled tube column
Elliptical section
Slenderness ratio
Stiffness
Strength
Self-compacting concrete

ABSTRACT

This paper presents the experimental results and observation of elliptical concrete filled tube (CFT) columns subjected to axial compressive load. A total of twenty-six elliptical CFT specimens including both stub and slender composite columns are tested to failure to investigate the axial compressive behaviour. Various column lengths, sectional sizes and infill concrete strength are used to quantify the influence of member geometry and constituent material properties on the structural behaviour of elliptical CFT columns. As there is no design guidance currently available in any Code of Practice, this study provides a review of the current design rules for concrete filled circular hollow sections in Eurocode 4 (EC4). New equations based on the Eurocode 4 provisions for concrete filled circular hollow sections were proposed and used to predict the capacities of elliptical CFT columns.

1. Introduction

The composite CFT column is well renowned for its strength, good ductility and energy absorption capacity in earthquake. This type of columns has also been proven to be economical due to rapid construction, as the external steel tubes may act as permanent and integral formworks which lead to reduction in labour costs, materials and construction time. The orientation of steel and concrete materials in a CFT column is also beneficial in terms of enhancing the columns' stiffness and bending strength, as the steel tube has a greater elastic modulus owing to the fact that the element is situated furthest from the centroid of the cross section [1].

Elliptical hollow section (EHS) is a relatively new cross-section that has been introduced in the UK by CORUS. It offers an additional choice to structural designers for its structural efficiency and to the architects for its appearance. This section may provide greater bending capacity compared to the circular hollow section with identical area and weight, due to its strong and weak axis directions [2]. However, currently there is limited understanding concerning the structural behaviour of elliptical CFT columns. Presently, the design for the compressive members with elliptical section shape has not been covered by any Code of Practice, Specification or Standard. However due to the increases in the use of such hollow section shape, broad study has been conducted to provide an insight to the behaviour of this form of structures.

Extensive researches have been carried out on short EHS columns [3–10]. These included experiments on typical steel hollow sections with different wall thicknesses, normal to high concrete infill strength, various loading cases including loading compositely, loading on concrete core only and loading through steel section only. From these studies, the effect of the strength of concrete infill and wall thickness of steel hollow sections on the structural behaviour has been highlighted. Furthermore the comparison and analyses showed that the effect of steel tube wall thickness was especially sensitive in composite columns with normal strength concrete as the capacity of the columns depends on the effect of confinement that is provided by the steel tube. When the concrete strength increases, the influence of wall thickness becomes less significant.

Researches on the ultimate strengths of elliptical carried out by the authors with the square and circular CFT columns carried out by Lam and Williams [4], and Giakoumelis and Lam [11] showed that the circular CFT columns were better than elliptical CFT columns due to the circular hollow section providing stronger confinement to the concrete core, higher axial load may be achieved by elliptical CFT columns as compared to square and rectangular CFT columns. This attributes to the curved section shape of the elliptical tube that offers more circumferential tension which in turn provides a higher confinement to the concrete core.

Further investigation on elliptical CFT columns carried out by Yang et al. [12] indicated that the wall thickness of the tube did affect the axial compressive behaviour of this type of composite columns. Inclined shear failure on the concrete infill was observed in composite columns with smaller wall thickness of the steel sections due to less

* Corresponding author. Tel.: +44 1274234052; fax: +44 1274234525.
E-mail address: d.lam1@bradford.ac.uk (D. Lam).

0143-974X/$ – see front matter © 2013 Elsevier Ltd. All rights reserved.
http://dx.doi.org/10.1016/j.jcsr.2013.04.002

confinement when compared to composite columns with greater wall thickness of the steel sections. The relationship between cylinder strength and concrete contribution ratio (CCR) demonstrated that the wall thickness of the steel sections has direct contribution to the increase capacity of the concrete infill. Experimental study on stub elliptical CFT columns carried out by Zhao and Packer [13] considered both normal to high strength SCC concrete and adopted different loading conditions. The simple superposition approach in predicting the ultimate capacity of CFT stub columns with elliptical hollow section (EHS) as an equivalent of RHS was proposed to predict the capacity of elliptical CFT columns.

Experimental study and numerical modelling on EHS carried out by Gardner and Ministro [14] included geometric features, non-linear material properties and initial geometric imperfections. Several amplitudes of initial geometric imperfections were considered and it was found that the structural behaviour of hollow sections was very sensitive to the level of imperfection; however the ultimate load was relatively less sensitive to the amplitude of the imperfection. Parametric studies with different section aspect ratios and varying slenderness for elliptical hollow sections were also carried out following the satisfactory validation of numerical method against experimental results [15]. Preliminary effective area formulation for slender EHS was also proposed in their study.

An investigation on local buckling behaviour of the EHS columns in compression was performed by Zhu and Wilkinson [8]. In their study the term "equivalent CHS" was used to model the local buckling of EHS. The diameter term, D in theoretical elastic buckling load of a circular hollow was replaced by D_1^2/D_2 which represents the major and minor diameters of the ellipse. It was confirmed that the use of an equivalent CHS was a reasonably good predictor for the capacity of slender sections and the deformation capacity of compact sections.

Numerical studies on elliptical CFT columns have been carried out by the authors [6,7], a new confined concrete model were developed for the elliptical CFT columns. However, as for columns with high strength concrete (HSC), the confined concrete properties has little effect to the behaviour. This is due to the increment of the compressive strength and stiffness of high concrete has little confinement effect at the failure stage as the steel hollow section has already yielded. Further numerical simulation on elliptical CFT columns was carried out by Dai and Lam [6]. Based on the comparison and analysis against experimental results available, a modified stress–strain model was proposed. In this model, a 'quick softening' section was introduced to consider the effect of elliptical geometric feature. This modified model has been used successfully in prediction of axial compressive load and failure modes of stub elliptical CFT columns.

2. Experimental specimens and test setup

A total of twenty-six CFT column specimens including stub and slender members were constructed using commercially available 150 × 75 × 4 mm and 200 × 100 × 5 mm elliptical steel hollow sections. The length of stub column was taken as two times the major outer diameter to ensure that they were sufficiently short and would not fail with overall buckling but long enough to have a representative residual stress pattern [14]. Three different lengths were chosen for long column specimens in order to examine the influence of slenderness on column strength. The D/t ratios of elliptical CFT columns tested was 37.5 and 40 and the slenderness ratio, L_{cr}/i_z, of long columns ranged from 16 to 143. The value of D was taken as the larger diameter and the critical buckling length, L_{cr} is taken from the centre to the centre of the end supports.

The selected column specimens were classified into four series depending on the length (height) as summarised in Table 1. Series I represents the stub columns, in which column length is of 300 mm or 400 mm according to the section dimensions. Series II, III and IV represent long columns with the lengths of 1500, 1790 and 2500 mm respectively. Before testing, each selected specimen was labeled according to its length, section size and nominal concrete strengths for easy identification. For instance, for label CIII-150-C30, the first letter and roman number, CIII represents column from series III with column length equaled to 2500 mm and the numbers 150 in the middle of the label represents the major outer diameter of steel hollow section 150 × 75 mm. The ending part C30 indicates the concrete infill grade.

Table 1
Measured dimension of elliptical hollow tubes and concrete properties.

	Specimen ID	2a mm	2b mm	L mm	t mm	b/t	f_{cu}	f_{ck}
Series I	CI-150 h	150.3	75.2	299.5	4.2	9.0	–	–
	CI-150-C30	150.1	75	300.0	4.1	9.1	47.1	37.4
	CI-150-C60	150.2	75.1	301.0	4.0	9.4	62.1	36.2
	CI-150-C100	150.1	75.2	299.0	4.2	9.0	105.9	90
	CI-200 h	197.8	100.1	400	5.2	9.6	–	–
	CI-200-C30	197.8	100.1	398	5.1	9.8	48.3	35.2
	CI-200-C60	197.5	100.2	398	5.1	9.8	66.5	41.6
	CI-200-C100	197.4	100.1	398	5.1	9.8	115.8	72.3
Series II	CII-150-C30	150.9	75.4	1497	4.0	9.4	26	19.8
	CII-150-C60	150.4	75.2	1498	4.1	9.2	64.1	52.2
	CII-150-C100	150.3	75.2	1496	4.1	9.2	90.8	77.5
	CII-200-C30	197.5	100.2	1499	5.2	9.6	29	26.7
	CII-200-C60	197.4	100.1	1498	5.1	9.8	64.1	41.8
	CII-200-C100	197.7	100.1	1498	5.1	9.8	90.8	71.1
Series III	CIII-150-C30	150.5	75.4	1785	4.1	9.2	20	13
	CIII-150-C60	150.7	75.2	1785	4.2	9.0	64.5	50
	CIII-150-C100	150.7	75.4	1786	4.1	9.2	99.9	72.3
	CIII-200-C30	197.6	100.2	1785	5.1	9.8	42	29.4
	CIII-200-C60	197.7	100.1	1786	5.1	9.8	63	40.6
	CIII-200-C100	197.3	100.0	1786	5.2	9.6	97.7	76.4
Series IV	CIV-150-C30	150.0	75.1	2500	4.2	8.9	23	18.4
	CIV-150-C60	150.2	75.0	2502	4.0	9.4	62.9	53.5
	CIV-150-C100	150.1	75.0	2501	4.1	9.1	99.9	72.3
	CIV-200-C30	197.5	100.3	2498	5.2	9.6		
	CIV-200-C60	197.8	100.1	2499	5.1	9.8	58.6	49.8
	CIV-200-C100	197.7	100.1	2498	5.1	9.8	101.1	73.8

2.1. Material properties

Self-compacting concrete (SCC) was chosen for the infill concrete to avoid the necessity for compacting and to provide the ease of casting as the SCC possesses high workability and achieve full compaction by self-weight [16]. Different SCC concrete mix specifications were tried to achieve nominal concrete cube strength of 30, 60 and 100 MPa. There is no reinforcement in the concrete core. Additional addictive such as super-plasticiser and pulverised fuel ash (PFA) were added into the concrete mixture to improve the fresh concrete properties.

SCC is susceptible to quantity and material fluctuations therefore tests on fresh and hardened properties were conducted to evaluate its characteristics and the quality control process until an acceptable mix specification was found. Table 2 gives a summary of the governing parameters adopted for fresh SCC concrete tests [16] (slump flow, flow time and stability sieving). The strength of SCC was determined by cube (100 × 100 × 100 mm) and cylinder (Ø150 × 300 mm) specimens. These specimens were cured with the test specimens. For each column specimen, the average cube strength and cylinder strength of the concrete core are summarised in Table 1.

Table 2
Segregation analysis.

Tests	Requirement
Slump flow	SF2 class: 660–750 mm
T500	VS2 class: with 3.5–6.0 s
Sieve segregation test	$5\% \leq r \leq 15\%$
	Satisfactory segregation resistance

The mechanical properties of steel material were determined by tensile coupon tests. Typical stress-strain curves and parameters were given in Fig. 1 and Table 3. Coupons were taken from the flatter side of the elliptical steel hollow section and prepared in accordance with EN 100002-1.

2.2. Test set up

All columns were tested in a vertical position subjected to axial compression as shown in Fig. 2. For the long column tests, pinned end joints were constructed by using groove plates and a steel ball in each end to allow free rotation at both ends. Before the test, the top surface of each specimen was levelled and ground. A layer of high strength mortar was capped at the top of the concrete core to ensure the axial load is applied to the composite section uniformly. For stub column specimens, both ends were capped by the steel plates to ensure full contact between specimens and end bearings whereas for long column specimens, only the bottom end of the specimen was welded to the steel plate to facilitate the placing of concrete while the other end was secured by a slotted plate as shown in Fig. 2. When the columns had been placed in the test rig, a small load was applied to hold the specimen upright, and then the specimen was carefully centralised using plumb bulb, laser and spirit level. Before the test began, pre-load was conducted to ensure that the loading was applied concentrically. Top and bottom strain gauges were used to assess the uniformity of the load. The measurements of both strain gauges were considered by comparing to their average strain recording to ensure the load was applied uniformly. Reasonable adjustment was made until the differences between measured strain and their average value became less than 5% [17]. The experimental results regarding failure mode, circumferential strain distribution, load-deformation behaviour and evaluation of the strength of the columns were recorded during the course of the testing. Displacement control with the rate of 0.2 mm/min was used so that the local buckling behaviour of the CFT columns could be carefully observed. To study the failure modes and the compressive behaviour of the tested columns, strain gauge was bonded to the outer surfaces to record the extreme fibre strains and linear displacement transducers (LVDT) were fixed to monitor longitudinal shortening and lateral displacement of the column. Three sets of LVDTs were set up at positions along the length of each column, i.e. the upper, mid-height and lower length of the specimens.

3. Experimental results and observation

3.1. Axially compressive capacity

Fig. 3 shows the axial compressive load vs. shortening relationships of the stub column specimens tested. The columns behaved in a stiff manner at the beginning of loading till the ultimate load approached, then a drop in the capacity of the CFT stub columns characterised the crushing of the concrete core and followed by the local buckling of the steel section. The CFT stub columns displayed a superior performance compared to steel hollow sections in both axial compressive strength and initial stiffness. It appears that with the increase in concrete infill strength, the initial stiffness of composite columns also increased although in some cases it is less evident. The specimen failed after the maximum load is reached, it shows that the higher the infill concrete strength, the steeper the drop in strength. The horizontal plateau in the curves after the peak loads indicated that these columns were able to maintain the load before they failed completely. It was observed that the ultimate strength of all stub CFT stub column specimens were achieved after the local buckling and steel yielding occurred. This indicates that a CFT stub column is able to sustain further loading after the steel has yielded as the result of steel strain-hardening.

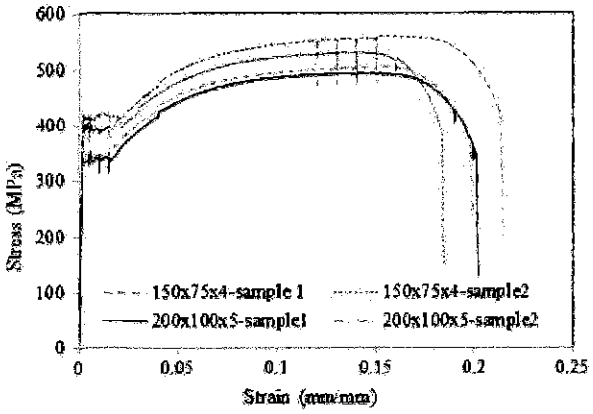

Fig. 1. Coupon tests results.

Table 3
Steel properties of the EHS.

Sample	Section size	f_y (MPa)	f_u (MPa)	ε_y με	E_s (N/mm^2)
1	150 × 75 × 4	431.4	529.4	2000	201,000
2		417.3	504.9		201,000
3	200 × 100 × 5	347.9	468.1	2000	205,000
4		375.5	477.7		213,000

Locally outward bulge formed before the steel reached its yield strain in some cases, however, the bulges did not seem to cause the CFT stub columns to lose their stiffness and strength immediately. The occurrence of local bulge observed in all CFT specimens was attributed to the force of local crushed concrete on the steel wall, in which the bulge grew in conjunction with the increasing load and resulted in the increase of the lateral movement of steel section wall that was being pushed out by dilatation of the concrete core. In the case of hollow columns, cases CI-150-h and CI-200-h, it was observed that the local failure occurred before the maximum load reached. Table 4 summarises the maximum load of all stub column specimens.

Fig. 4 shows the axial compressive load vs. axial shortening of long column specimens tested. It was noticed that after the maximum load reached, the gradient of the descending branches of the displacement curve are very steep. Unlike stub CFT columns, the maximum capacity of these long columns was governed by the global buckling response. It was observed the global buckling also caused higher stress concentration at the middle height region where the lateral deflection and strains increased rapidly as the maximum load was approaching. As expected; global buckling deformation was observed in all of the specimens and this consistency indicated that the homogeneity of the concrete inside the steel tubes and shown that SCC concrete may be used for concrete filled tubular members. Steep descending branches can be observed after these columns reached their peak loads from the load-lateral displacement relationships shown in Fig. 5, where the lateral displacement were recorded at the middle height of the columns. All the long column specimens failed elastic-plastically and the values of plastic strain in steel tube were small.

Accompanying the global buckling deformation, sign of local buckling could be observed for some column specimens. Generally it occurred before the steel is yielded and the maximum load was reached. Although some local buckling did occur, however, at that stage the columns remained vertical against the lateral deflection. Significant lateral displacement was only observed after the maximum load was achieved indicating that long CFT columns are capable in resisting additional load with the contribution from the concrete infill.

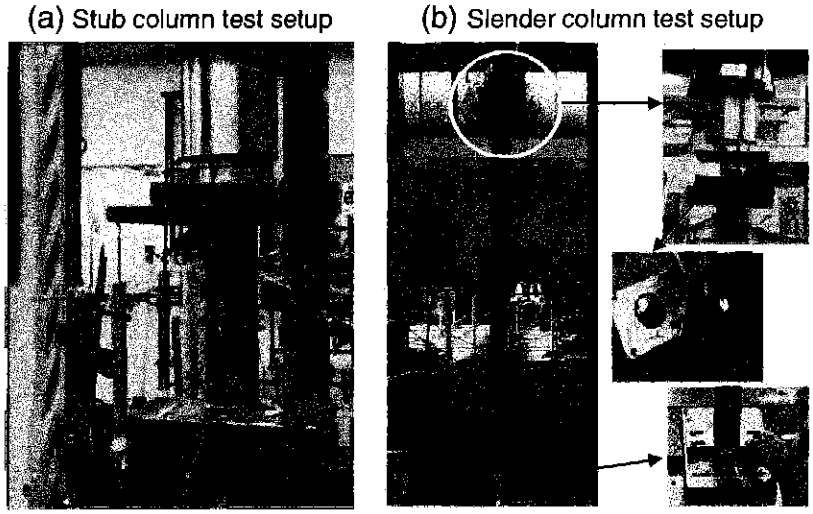

Fig. 2. Typical test set-up for stub and slender CFT columns.

3.2. Failure modes

Figs. 6 and 7 present the final deformation and failure modes of stub column specimens. As expected, a pattern of inward and outward bulges obviously occurred in stub hollow section column but the inward bulges were prevented by the presence of the concrete core in the concrete filled stub columns. The aggravated outward local buckling was exhibited particularly at the longer side wall and seemed to be affected by the strength of the concrete infill. Rings forming at both ends were observed in columns with normal strength concrete (NSC), while shear failure or splitting occurred in specimens with higher strength concrete (HSC) (Fig. 6). The specimens were cut to show that splitting due to the massive shear failure causing a longitudinal crack cutting straight across the concrete core could deal to the characteristics of SCC. (Fig. 7) SCC contains higher fine material and less coarse aggregates to minimise friction in order to ensure appropriate workability but this may affect the mechanical bond of the hardened concrete.

Unlike the stub CFT column members tested, the failure mode of a slender concrete filled steel tube column is characterised by the global buckling. Fig. 8 presents the final deformation for slender CFT columns with different column lengths (1.5 m, 1.8 m, and 2.5 m). As shown in Fig. 9, although the compressive crack developed in the concrete core, the core remained intact and contained by the steel tube due to the confinement interaction. Tension crack was observed in HSC cores. However for the specimens in Series IV, no concrete crushing is observed at the mid-length section (Fig. 9d).

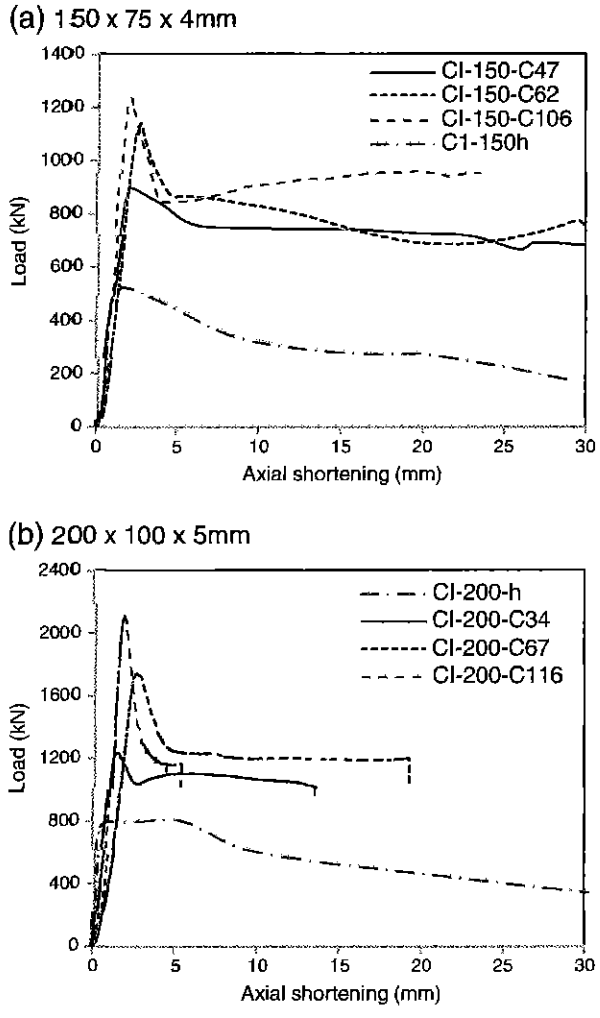

Fig. 3. Load-axial shortening relationship of stub column.

4. Discussion on compressive behaviour of CFT columns

4.1. Interaction between concrete core and steel hollow section

The concrete infill contributes substantially to the load bearing capacity of the CFT columns as illustrated in Figs. 3 and 4. In comparison to the steel hollow section columns, the strength of the stub CFT

Table 4
Summary of maximum load and ductility index for stub columns.

	Specimen ID	P_u (kN)	P_{CFT}/P_H	DI	SI
Series I	CI-150 h	525	–	–	–
	CI-150-C47	900	1.71	2.78	0.96
	CI-150-C62	1139	2.17	1.41	1.14
	CI-150-C106	1239	2.36	1.36	0.87
	CI-200 h	810.7	–	–	–
	CI-200-C34	1232	1.52	1.74	1.01
	CI-200-C67	1737	1.41	1.39	1.15
	CI-200-C116	2116	1.22	1.23	1.07

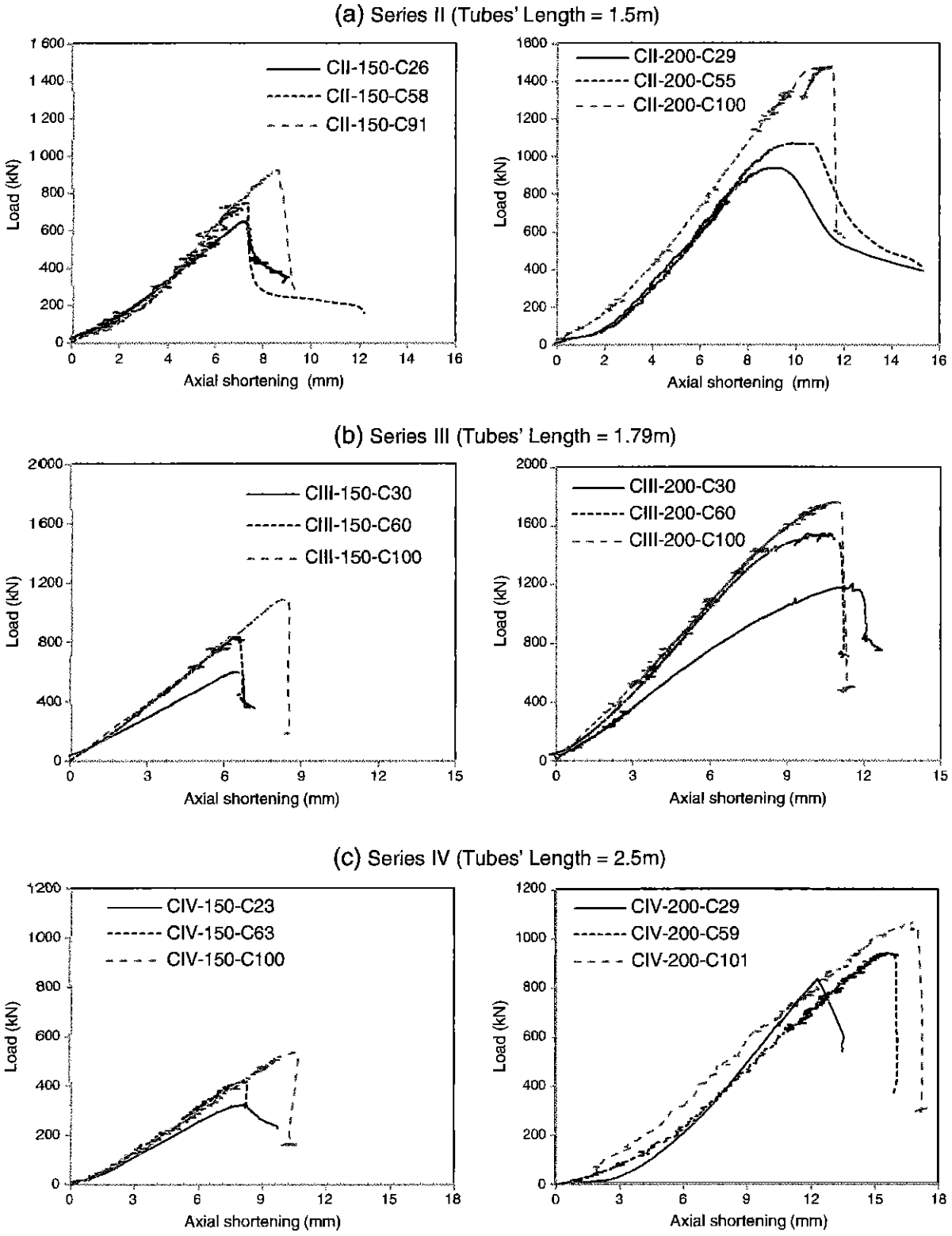

Fig. 4. Load vs. axial shortening of elliptical CFT columns.

columns is over 50% higher than the capacity of the steel section alone which is attributed to the presence of concrete core. The presence of the concrete core also increases the flexural rigidity as demonstrated by the slope of the curves. The increase in strength due to concrete infill is given by the ratio of P_{CFT}/P_H for the stub columns. For tested stub columns, the value of this ratio ranges from 1.41 to 2.36 as shown in Table 4. However it should be noted, for stub CFT columns with high concrete strength infill, confinement effect should not be considered. HSC infill exhibited smaller confinement effect due to the low dilatation of the concrete which prevented the development

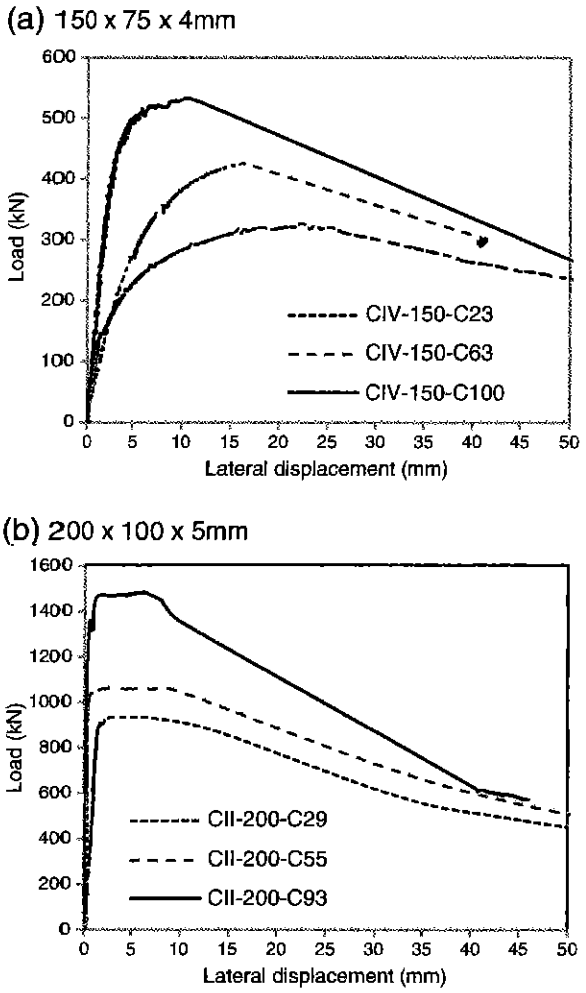

Fig. 5. Load vs. lateral displacement at mid-height for Series II and IV.

of confinement effect. Confinement is only achieved when the micro cracking of the concrete core increases to enable the concrete infill to expand and exert lateral compressive stress on the steel tube. However, with the increase of in the concrete strength, the stiffness of the concrete also increases, therefore resulting in less lateral expansion of concrete core, which is also the reason the confinement gives little effect to the high strength concrete infill. In addition, the

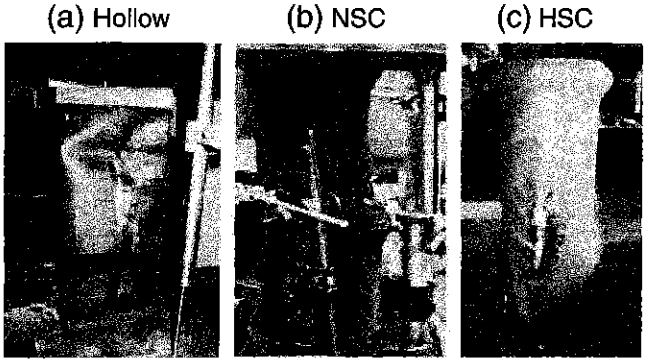

Fig. 6. Typical failure modes of elliptical short column.

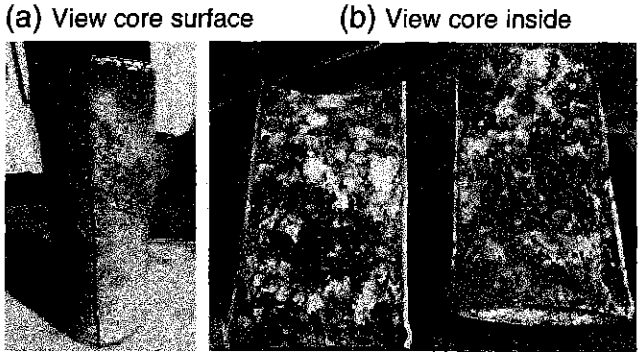

Fig. 7. HSC core failures.

mechanical bonding strength of SCC is relatively weak and this resulted in lower shear strength due to the reduced shear friction.

For slender CFT columns, columns with lower concrete strength exhibited greater mid-height lateral deflection than that of columns with higher concrete strength at any given level of load. This may be attributed to the fact that the HSC has higher modulus of elasticity. As shown in Fig. 10, the influence of concrete strength on the longitudinal stress–strain curves can be seen and the impact of varying concrete strengths on the capacity and stiffness of the columns are demonstrated. In general, the strength and stiffness of elliptical CFT columns increase as the concrete strength increases. Specimens with higher strength concrete have larger elastic rigidity in the elastic stage as the initial elastic modulus of the concrete increases with the concrete strength. The presence of the concrete infill also increases the flexural rigidity as shown by the slope of the curves. The average stress-strain relationship is used to eliminate the influence of specimen dimension and obtained by dividing the load by the cross-sectional area of the elements ($A_s + A_c$).

4.2. Effect of slenderness to compressive behaviour

The effect of slenderness ratio on column axial capacity was examined by considering the specimens with similar concrete strength and sectional dimension but different lengths is shown in Fig. 11. As the length of the columns increases, the columns with higher slenderness had a lower maximum load than columns with lower slenderness and the load reduced quickly once the ultimate load was reached. The reduction of compressive capacity due to flexural buckling of 1.5 m CFT column to 2.5 m CFT column was up to 50%. Column with higher slenderness was shown to have greater flexibility which resulted in greater mid-height displacement at any given load and lower stiffness compared to column with lower slenderness due to instability.

As expected, all long column specimens failed at mid-height with global buckling occurring around the major axis. This finding runs parallel with the finding of the hoop strains at major axis vertices, in which the strains were almost constantly larger than those at the minor axis vertices.

4.3. Ductility Index (DI) and compressive behaviour

Ductility is defined as the ability to possess non-linear deformation under loading [18]. It is characterised by a large plastic deflection without a considerable loss of load-bearing capacity [19]. In this paper, the ductility behaviour is assessed by means of a ductility index in which the axial displacement results were considered. The ductility index (DI) here is defined as the ratio of top end vertical displacement at which the strength of the specimen dropped to 85% of the ultimate load to the end vertical displacement at the ultimate

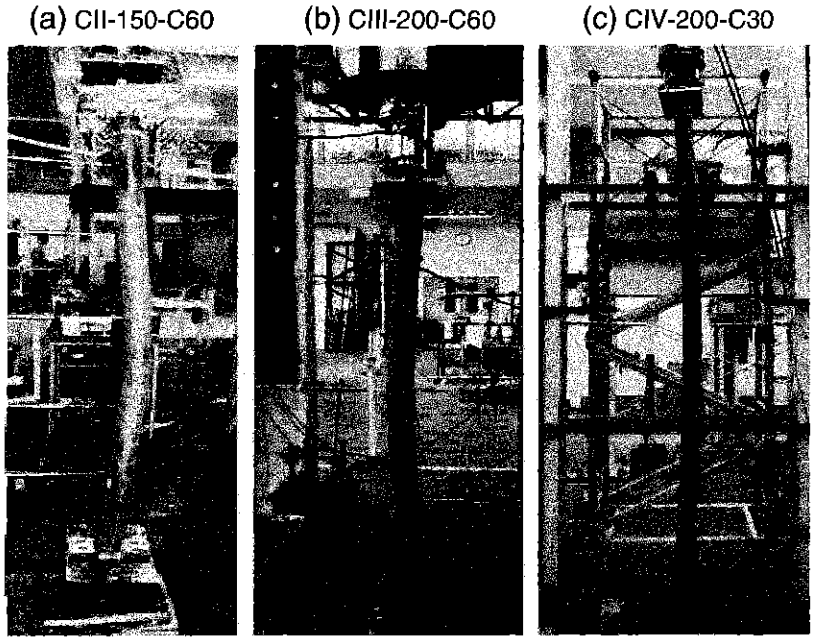

Fig. 8. Deformation of long CFT columns.

load (Eq. (1)). The values of DI for all tested specimens are listed in Tables 4 and 5.

$$DI = \frac{\Delta_{85\%}}{\Delta_u} \tag{1}$$

It can be seen from Tables 4 and 5 that the stub columns exhibit a remarkable ductility and the ductility index ranges from 1.23 to 2.78, which is significantly higher than that of the long columns whose DI value ranges from 0.95 to 1.12. This is due to the slender composite columns were failed by global buckling, the plasticity of steel tube material and the confinement effect of concrete core were not fully developed. As expected, the ductility of stub columns with very high strength concrete infill is smaller than that for stub columns with normal strength concrete infill. This is understood as the brittleness of concrete increases as the strength increases. For the slender columns, the ductility index decreases as the concrete strength increases. The higher compressive strength concrete has less micro-cracking resulting in less lateral expansion, which accordingly leads to less restrain offered by the steel tube. Consequently, the concrete experiences less confining pressure and affects the columns' ductility and resistance. Furthermore, the load of columns with HSC tends to drop quickly after the peak load has been achieved and there is no obvious ductility improvement.

5. Analysis and design to Eurocode 4

Eurocode 4 (EC4) covers the design rules for encased, partially encased and concrete-infill columns both with and without reinforcements. The code applies to the column with steel grades S235 to S460

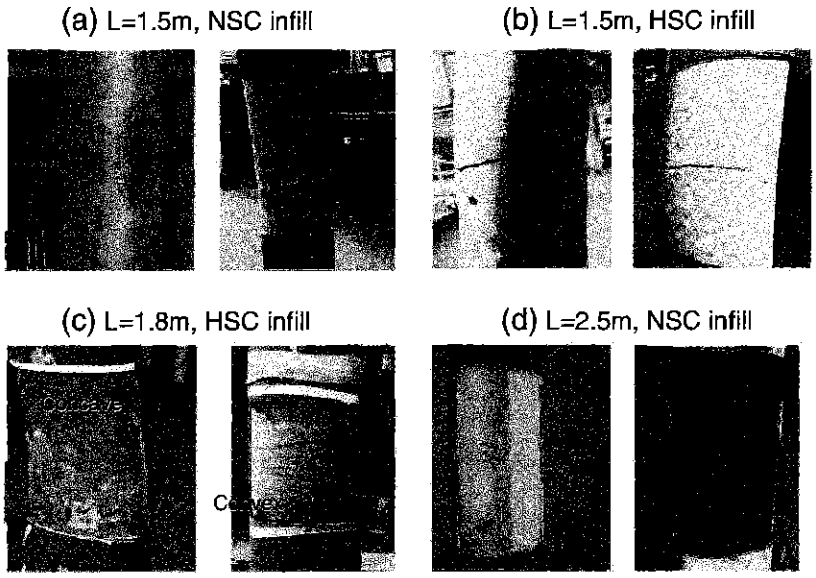

Fig. 9. The removal of steel envelope.

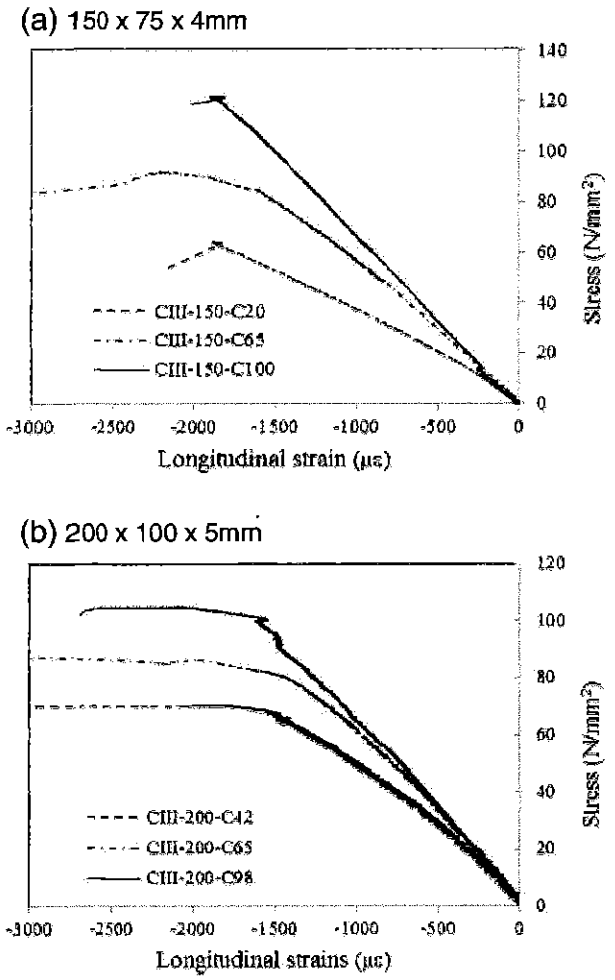

Fig. 10. Stress–strain relationship curves of long columns.

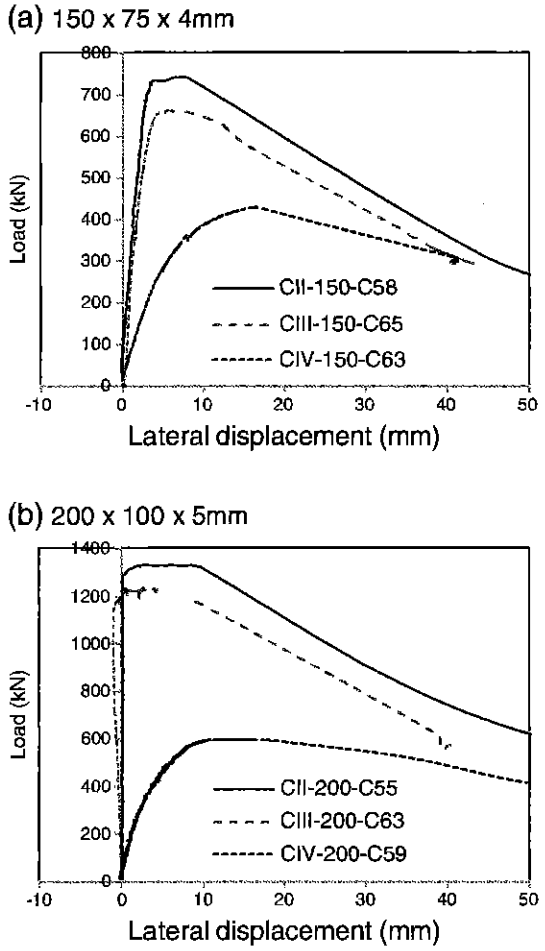

Fig. 11. Load to mid-height lateral displacement relationships for columns with various lengths.

and with the normal weight concrete of strength classes C20/25 to C50/60. The simple design and calculation method provided in the EC4 is adopted in this study to check their feasibility of application to elliptical CFT composite columns with the buckling curves given in Eurocode 3 (EC3) for steel columns. The resistance of the cross-section is calculated by assuming a fully plastic cross-section, the load of which is distributed reasonably between the steel and the concrete sections.

Using the EC4, The resistance of stub CFT columns was calculated as in Eqs. (2) and (3). Eq. (2) can be applied to composite CFT columns with the confinement effect neglected, but the coefficient of 0.85 in the expression is replaced by 1.0 in the case of concrete filled section. On the other hand, Eq. (3) considered the contribution of confinement provided by the tube in CFT columns.

$$N_{pl,RK(1)} = A_s f_y + 0.85 A_c f_{ck} \tag{2}$$

$$N_{pl,RK(2)} = \eta_s A_s f_y + \left[1 + \eta_c \left(\frac{t}{D}\right)\left(\frac{f_y}{f_{ck}}\right)\right] A_c f_{ck} \tag{3}$$

where η_s is a factor to reduce the tube strength to account for hoop stress whilst η_c in the equation indicates the effect of confinement in the concrete strength. The diameter, D was taken as an equivalent diameter for elliptical section or, $D_e = 2a^2/b$ in the case of elliptical tube. In this study, A_s and A_c were calculated as in Eqs. (4)–(6). The area of elliptical steel hollow section, A_s, was based on the study by Chan and Gardner [15].

$$A_c = \pi(a-t)(b-t) \tag{4}$$

$$A_s = P_m \times t \tag{5}$$

Table 5
Summary of maximum load and ductility index for slender columns.

	Specimen ID	P_u (kN)	DI
Series II	CII-150-C26	650.8	1.04
	CII-150-C58	742.8	0.97
	CII-150-C64	836	1.02
	CII-150-C91	923.2	1.01
	CII-200-C29	938.4	1.12
	CII-200-C55	1064	1.10
	CII-200-C93	1480	1.00
Series III	CIII-150-C20	483.8	1.06
	CIII-150-C65	663.2	1.01
	CIII-150-C100	871.2	1.02
	CIII-200-C42	967.5	1.04
	CIII-200-C63	1237	1.06
	CIII-200-C98	1411.2	1.01
Series IV	CIV-150-C23	326.6	1.08
	CIV-150-C63	427	1.01
	CIV-150-C100	547.4	0.95
	CIV-200-C29	839	1.10
	CIV-200-C59	947	1.00
	CIV-200-C101	1072.3	1.01

$$P_m = \pi(a_m + b_m)(1 + 0.25h_m) \quad (6)$$

where P_m is the mean perimeter and t is the thickness of the elliptical section whilst $a_m = \frac{2a-t}{2}$, $b_m = \frac{2b-t}{2}$ and $h_m = \frac{(a_m-b_m)^2}{(a_m+b_m)^2}$. The values of 2a and 2b are taken as the larger and smaller outer diameters of the elliptical section.

Further assessment on the capacities of long CFT columns were based on the buckling curves. The squash load of the corresponding long columns was reduced by the reduction factor, χ which takes into consideration the influence of buckling in terms of the relative slenderness ratio and relevant buckling curve. The design load of a slender column may be:

$$N_{Ed} \leq \chi \cdot N_{pl,Rd}$$

The reduction factor χ for the relevant buckling mode is a function of the relative slenderness $\overline{\lambda}$, which is determined from:

$$\chi = \frac{1}{\varphi + \left[\varphi^2 - \overline{\lambda}^2\right]^{0.5}} \leq 1 \quad (8)$$

where:

$$\varphi = 0.5\left[1 + \alpha(\overline{\lambda} - 0.2) + \overline{\lambda}^2\right] \quad (9)$$

The imperfection factor α corresponds to the relevant buckling curve and the relative slenderness $\overline{\lambda}$ for the plane of bending being considered is given by:

$$\overline{\lambda} = \sqrt{\frac{N_{pl,Rk}}{N_{cr}}} \quad (10)$$

where, $N_{pl,Rk}$ is the resistance of the cross section to compressive load and N_{cr} is the axial elastic critical load. For the determination of the relative slenderness $\overline{\lambda}$ and the elastic critical force N_{cr}, the characteristic value of the effective flexural stiffness $(EI)_{eff}$ of the cross section of a composite column should be calculated from:

$$EI = E_a I_a + 0.6E_{cm} I_c + E_s I_s \quad (11)$$

where E_{cm} is the modulus of elasticity of infill concrete, I_a, I_c, and I_s are the second moments of area of the structural steel section, the un-cracked concrete section and the reinforcement for the bending plane being considered. As mentioned previously, there is no reinforcement for these composite columns and therefore the $E_s I_s$ term may be ignored here.

As shown in Table 6, the column strength, P_u obtained from the experiments are compared with the un-factored design column strengths P_{EC4} calculated using the EC4. The ratios of P_u/P_{EC4} are summarised in Table 6 for stub and long columns respectively for all columns, the ratio of P_u/P_{EC4} is greater than unity except the exemption for a few specimens, this suggested that the EC4 prediction is in the safe side. In this research, the equivalent diameter D_e was used in the calculation. From this study, the considerations of equivalent diameter of $2a^2/b$ for elliptical CFT columns gave a reasonably estimate of the elliptical CFT columns capacities. The influences of concrete enhancement, steel reduction due to biaxial effects and column slenderness were incorporated in the design rules of circular concrete-filled tubes which is also applicable to the elliptical CFT columns.

Table 6
Comparison of maximum loads by experiment and EC4 prediction for stub CFT columns.

Specimen ID	P_u	P_{EC4}	P_u/P_{EC4}
CI-150-C47	900	909.6	1.0
CI-150-C62	1139	968.2	1.2
CI-150-C106	1290	1299.3	1.0
CI-200-C34	1232	1050	1.2
CI-200-C67	1737	1298.2	1.3
CI-200-C116	2116	1710.8	1.2
		Average	1.1
		COV	0.1

Table 7
Comparison of maximum loads by experiment and EC4 prediction for slender CFT columns.

Specimen ID	P_u	P_{EC4}	P_u/P_{EC4}
CII-150-C26	520.6	532.2	0.98
CII-150-C64	742.8	627.8	1.18
CII-150-C91	923.2	679.7	1.36
CII-200-C29	938.4	1018.3	0.92
CII-200-C55	1064	1181.6	0.9
CII-200-C93	1480	1431.3	1.03
CIII-150-C20	483.8	444.4	1.09
CIII-150-C65	663.2	513.6	1.29
CIII-150-C100	871.2	536.5	1.62
CIII-200-C42	967.5	993.9	0.97
CIII-200-C63	1237	1078.4	1.15
CIII-200-C98	1411	1311.9	1.08
CIV-150-C23	326.6	284.9	1.15
CIV-150-C63	427	297.8	1.43
CIV-150-C100	547.4	311.1	1.76
CIV-200-C29	839	733.4	1.14
CIV-200-C59	947	818.5	1.16
CIV-200-C101	1072	875	1.23
		Average	1.19
		COV	0.19

Previous research on CFT columns has often been restricted to short specimens. In the case of long columns, there is little evidence of an increase in concrete strength owing to the confinement. In the EC4 method, the confinement for slender columns was assumed to be insignificant when the non-dimensional slenderness $\overline{\lambda}$ is larger than 0.5. When the non-dimensional slenderness is exceeded 0.5, the factors η_s and η_c should be taken as 1 and 0 respectively.

Table 7 summarises the ratio of experimental capacity, P_u to EC4 predicted capacity, P_{EC4}. The average ratio is 1.19 with a COV of 0.19. With exemption of specimen CII-200-C55, where the experimental capacity was 10% lower than EC4 prediction, all the results were above the 10% margin. In general, despite ignoring the strain hardening effect of the steel material, the EC4 predicted results are fairly close to those measured from the experiment. Although the current EC4 equations under predict the capacity of the composite

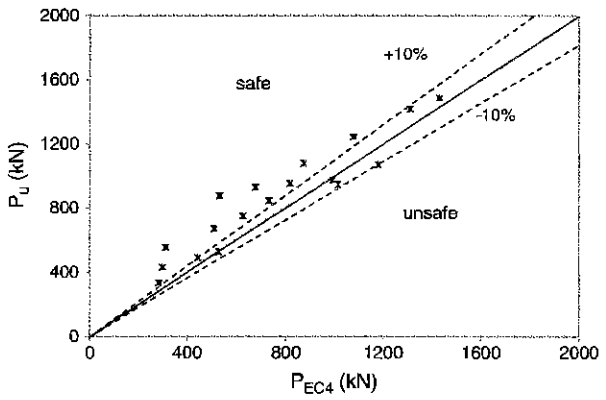

Fig. 12. Comparison of experimental ultimate loads and EC4 predicted loads.

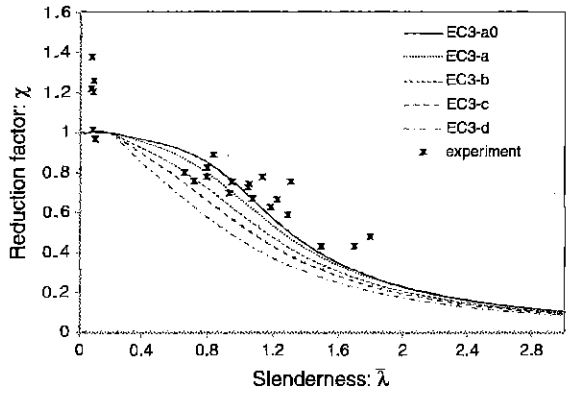

Fig. 13. comparison of normalised experimental loads to the EC buckling curves.

columns with HSC, it should note that HSC used in this research is not currently allowed in the current provision of EC4.

The maximum loads obtained from experiments and predicted by EC4 are also compared in Fig. 12, where the solid line represents the experiment results vs. predicted results by EC4 as 1.0. The other two dotted lines represent ± 10%. From Fig. 12, the results of most of the slender columns fall on the safe side, this showed that the proposed method has provided a reasonable estimation for this form of composite columns.

For the axially loaded CFT columns, the slenderness of the columns will generally determine whether the strength of the cross-section or instability of the member governing the load carrying capacity. In the case of long elliptical CFT columns under axial compression, the increase in strength due to confinement effect could be assumed. However due to the slenderness, the confinement effect could not develop fully. This indicates that the L/D ratio affects the degree of confinement as well as the load capacity. Lateral instability before any mobilisation of the confinement is more prominent for columns with higher L/D ratio.

Fig. 13 compares the experiment results against the non-dimensional slenderness and the buckling curves given in the Eurocode 3 (EC3). From Fig. 13, it can be seen that the EC3 buckling curve generally provides a lower bound to the experimental results. Almost all experimental points lay above the buckling curves; this indicates that the buckling curves are deemed safe for elliptical CFT columns, particularly for columns with higher slenderness. For concrete filled tube columns, buckling curve "a" with the imperfection factor, $\alpha = 0.21$ is used when the reinforcement ratio does not exceed 3%. Further analysis shows that the column curve is reliable in determination the influence of slenderness. The buckling curve 'a' agrees fairly well with the experimental data.

The reduction factor χ based on EC4 method is dependent on the relative slenderness $\bar{\lambda}$ of the columns and imperfection. It should be noted that these five buckling curves reflect the differences in imperfections including geometric imperfection, lack of verticality, straightness, flatness and accidental eccentricity of loading. Therefore the buckling loads for the under-predicted specimens can be seen depend not only on its slenderness ratio but also their mechanical properties of material. However, as most of the experimental failure load points lay above the EC3 buckling curve "a", therefore using these buckling curves for the slender elliptical CFT composite columns is conservative.

6. Conclusion

The research presented in this paper investigated the axial compressive behaviour of a series of elliptical concrete filled steel tube columns with two steel section sizes and various concrete strengths. Based on the comparison and analyses, the following conclusions may be made:

1) The confinement of steel hollow section to concrete core played an important role in enhancing the capacity and eliminating or delaying the occurrence of local buckling in stub composite columns.
2) The failure of stub concrete filled tubular columns was characterised by the local buckling on steel section wall and concrete crushing, but the failure of slender CFT columns was governed by the global buckling although at the middle height, local visible compressive crushing and tensile cracks were observed.
3) The axial compressive load capacity and ductility of a CFT column were sensitive to steel hollow section dimensions, concrete infill strength and the slenderness ratio. It appears that the ductility index decreased with the concrete infill strength increasing. In most cases, the compressive load of specimens experienced a steep "drop" after the ultimate load was reached. This may contribute to the brittleness of high strength concrete for slender columns while the over strength in the short column can be explained by the confinement of concrete core from steel tube.
4) The normal strength concrete column led to much ductile failure in comparison to the columns filled with high strength concrete, this is attributed to the fact that the high strength concrete is brittle and tensile fracture failure was found at tensile zone.
5) The failure mode of all slender column specimens was characterised by the overall flexural buckling however, in most cases local steel yielding occurred before the global buckling. This indicated local buckling did not reduce ultimate load capacity of the slender composite columns.
6) The increase in the column slenderness reduces the load carrying capacity of composite columns. The obvious explanation for this condition is that for the short columns the steel section was expected to exert a lateral pressure on the concrete core and resulted in increasing the capacity. The use of high concrete strength enhanced the load carrying capacity of the tested columns, but with a load–slenderness relationship decreasing at a higher rate compared to that of columns using normal strength concrete.
7) The EC4 method displays reliable results as the confinement effect was considered. The European buckling curves for steel columns can be considered as the basis of elliptical CFT column design.
8) This study also examined the applicability of design standards of EC4 for the design of elliptical CFT with high strength concrete infill. The principle limitation in EC4 code is the normal weight of concrete strength classes of C20/C25 to C50/C60. However, the utilisation of HSC could also be safely extended to predict the capacity of elliptical columns.

Acknowledgement

The authors would like to acknowledge the financial support provided by the Engineering and Physical Science Research Council in the UK (EP/G002126/1), Tata Steel and Drax Power Station for providing the steel specimens and PFA material used in this research project. The authors are also grateful to the Ministry of Higher Education of Malaysia and Universiti Tun Hussein Onn Malaysia for providing the financial support to the first author for her PhD study.

References

[1] Gourley BC, Tort C, Hajjar JF, Schiller PH. A synopsis of studies of the monotonic and cyclic behaviour of concrete-filled steel tube beam-columns. Structural Engineering Report No. ST-01-4. University of Minnesota: Institute of Technology; 2001.

[2] Packer AJ. Going elliptical.Modern Steel Construction, American Institute of Steel Construction; 200865–7 [March Issue].
[3] Lam D, Testo N. Structural design of concrete filled steel elliptical hollow sections. Composite Construction VI, Colorado USA; 2008.
[4] Lam D, Williams CA. Experimental study on concrete filled square hollow sections. Steel Compos Struct 2004;4(2):95–112.
[5] Yang H, Lam D, Gardner L. Testing and analysis of concrete-filled elliptical hollow sections. Eng Struct 2008;30(12):3771–81.
[6] Dai X, Lam D. Numerical modelling of axial compressive behaviour of short concrete-filled elliptical steel columns. J Constr Steel Res 2010;66(7):931–42.
[7] Jamaluddin N, Lam D, Ye J. Finite element analysis of elliptical stub CFT columns. In: Lam D, editor. Proceedings of the 9th International Conference on Steel Concrete Composite and Hybrid Structures (ASCCS 2009), Leeds, UK, 8-10 July 2009. Singapore: Research Publishing; 2009.
[8] Zhu Y, Wilkinson T. Finite element analysis of structural steel elliptical hollow sections in compression. Research Report No.R874. Australia: Centre of Advanced Structural Engineering, School of Civil Engineering, The University of Sydney; 2007.
[9] Zhao XL, Packer JA. Tests and design of concrete-filled elliptical hollow section stub columns. Thin-Walled Struct 2009;47(6–7):617–28.
[10] Testo N. Axial capacity of elliptical concrete-filled steel tube columns. Research Report. School of Civil Engineering, University of Leeds; 2007.
[11] Giakoumelis G, Lam D. Axial capacity of circular concrete-filled tube columns. J Constr Steel Res 2004;60(7):1049–68.
[12] Yang D, Lam D, Gardner L. Testing and analysis of concrete-filled elliptical hollow sections. Eng Struct 2008;30(12):3771–81.
[13] Zhao XL, Lu H, Galteri S. Tests of elliptical hollow sections filled with SCC (self-compacting concrete). Proceeding of the 5th International Conference on Advances in Steel Structures, Singapore; 2007. p. 979–84.
[14] Gardner L, Ministro A. Testing and numerical modelling of structural steel oval hollow sections. Research Report No.04-002-ST. London, U.K.: Imperial College; 2004.
[15] Chan TM, Gardner L. Compressive resistance of hot-rolled elliptical hollow sections. Eng Struct 2008;30(2):522–32.
[16] SCCEPG. The European guidelines for self-compacting concrete—specification, production and use. [online] Available at: http://www.efnarc.org/pdf/SCCGuidelines May2005.pdf; 2005. [Accessed 10 February 2012].
[17] Hanbin G, Tsutomo U. Strength of concrete-filled thin-walled steel box columns: experiment. J Struct Eng 1992;118(11):3036–54.
[18] Gopal SR, Manoharan PD. Experimental behaviour of eccentrically loaded slender circular hollow steel columns in-filled with fibre reinforced concrete. J Constr Steel Res 2006;62(5):513–20.
[19] Grauers M. Composite columns of hollow steel sections filled with high strength concrete. PhD. Thesis Division of Concrete Structures. Sweden: Chalmers University of Technology; 1993.